

Journal of Materials Chemistry A

Accepted Manuscript



This is an *Accepted Manuscript*, which has been through the Royal Society of Chemistry peer review process and has been accepted for publication.

Accepted Manuscripts are published online shortly after acceptance, before technical editing, formatting and proof reading. Using this free service, authors can make their results available to the community, in citable form, before we publish the edited article. We will replace this *Accepted Manuscript* with the edited and formatted *Advance Article* as soon as it is available.

You can find more information about *Accepted Manuscripts* in the [Information for Authors](#).

Please note that technical editing may introduce minor changes to the text and/or graphics, which may alter content. The journal's standard [Terms & Conditions](#) and the [Ethical guidelines](#) still apply. In no event shall the Royal Society of Chemistry be held responsible for any errors or omissions in this *Accepted Manuscript* or any consequences arising from the use of any information it contains.



Carbon materials as oil sorbent: A review on synthesis and performance

Received 00th August 20xx,
Accepted 00th August 20xx

DOI: 10.1039/x0xx00000x

www.rsc.org/

Shivam Gupta and Nyan-Hwa Tai*

The oil spill accidents have attracted scientists across the world to develop an immediate clean up technology because the spilled oil significantly affects the ecological and environmental system. Superhydrophobic and superoleophilic materials have shown potential application in the field of oil spill cleanup due to their outstanding absorption capabilities, high selectivity, chemical inertness and excellent recyclability. In this regard, carbon-based absorbents have been considered to be the best candidate as they possess high surface area, low density, excellent mechanical properties, good chemical stability, environmental friendliness and large pore volume. Carbon aerogels, graphene or carbon nanotubes (CNTs) coated sponges, carbon nanotube forests, graphene foams or sponges, carbon coatings, activated carbon, porous carbon nanoparticles and carbon fibers have been widely investigated for water filtration, water/oil separation, oil-spill cleanup, wastewater treatment, gas separation and purification. In this paper, the synthesis, applications and reusability of these carbon-based absorbents have been reviewed and their performance are compared.

Introduction

During the past few decades, there have been many oil spill accidents during extraction, transportation and storage of oil. Most of the oil spill accidents occurred in the sea as most of the oil transportation is done through the sea. In a massive oil spill accident in the Gulf of Mexico in 2010, approximately 4.9 million barrels oil spilled which outstripped the estimated 3.3 million barrels spilled into the Bay of Campeche by the Mexican rig Ixtoc I in 1979, previously believed to be the world's largest oil spill accident. This accident mostly impacted the marine species and seagrasses. Out of 322 species, 53 species were threatened and 29 were nearly threatened, including 16 species of sharks, and eight corals.¹ On December 2014, around 3000 barrels of oil spilled into the waters of the world famous Sundarbans nature reserve in Bangladesh after a collision between a tanker and another vessel. The oil spill blackened the shoreline, threatening trees, killing large numbers of sea birds, small fishes, dolphins and mammals because of its poisonous chemical constituents. In July 2015, on the beach of Kinmen County of Fujian province, a large black viscous oil patch was found with a total length of approximately one kilometre, as shown in Fig. 1. After primary investigation, it was concluded that the oil leaked from a ship and was immediately cleaned-up to protect the environmental and ecological system.

The oil spill in the sea is more dangerous than that on land as most of the oils floats on the sea surface and spreads over

wide areas by waves and wind so a rapid removal of spilled oil is required in order to prevent oil diffusion into a larger area. It can cause wide ranging environmental impacts such as physical damage to wildlife and their habitats, chemical toxicity, ecological changes and consequent elimination of rare species.³ The cleanup operations of oil spill greatly reduced the environmental loss and highly improved the economic resources of that area.⁴ Not only the oil spill accidents, but also the oil in industrial waste water is a problem for the ecosystem, which need to be solved.

To address these environmental issues arising because of oil spills, organic pollutants and industrial oily waste water, there are three different methods for oil spill cleanup, viz., mechanical⁵, chemical, and biological⁶. Generally, mechanical cleanup is the primary line of defense against oil spills. A typical mechanical cleanup system includes skimmers, booms, barriers and natural as well as synthetic sorbents. Chemical cleanup includes in situ burning⁷, the use of solidifiers and chemical dispersants⁸. Chemical dispersants help to break the slick of oil into droplets, which makes it easier for the oil to mix with water, and finally speed up its natural biodegradation. Biological methods or bioremediation involves bioremediation agents which make use of micro-organisms to alter, transfer and breakdown hydrocarbons of oil into other substances, such as fatty acids, carbonic gas and water.⁹⁻¹¹ Among these techniques, absorbent materials are considered to be one of the most effective approach because of their low production cost, easy fabrication, high selectivity, environmental friendliness and good recyclability. In this regard, the solid with surface possessing both superhydrophobicity (water contact angle (CA) greater than 150°) and superoleophilicity (oil contact angle less than 5°) are promising candidate because of

*Department of Materials Science and Engineering, National Tsing Hua University, Hsinch, Taiwan 300, ROC
E-mail: nhtai@mx.nthu.edu.tw*

its capacity of selective absorption of oils or organic solvents while repelling water completely.^{12,13} Although many natural absorbent materials, including sawdust,¹⁴ wool fiber,¹⁵ and zeolite¹⁶ have been widely used for the separation and removal of organics or oil from water due to their porous structures and high surface area, but these materials possess some major drawbacks such as low absorption capacities, poor recyclability and selectivity as they absorb both the water and the oil. Thus there is a growing demand to develop new porous materials and adsorbents with high absorption capacity, good selectivity, and environment-friendly properties. With these properties, they can be used to absorb, remove and transfer oil and organic pollutants from water. In 1964, Johnson and Dettre first studied the phenomenon of superhydrophobicity by using rough hydrophobic surfaces.¹⁷ In 1996, Kao Corporation also demonstrated artificial superhydrophobic surfaces using the material with fractal surface made of alkylketene dimer.¹⁸ After that, many different techniques have been reported to produce rough surfaces with superhydrophobicity. In recent years, numerous of oil sorbent materials such as organic-inorganic hybrid,¹⁹⁻²¹ crosslinked polymers and resins,²²⁻²⁵ fibers,²⁶ polymer gels,^{27,28} nanocomposites,^{29,30} silicas³¹ and carbon-based materials³²⁻³⁶ etc. have been developed extensively. Among these, carbon materials have been considered as the most suitable candidates for superhydrophobic and superoleophilic surfaces due to their high oil uptake capacity and environmental acceptability.

Theoretical aspect for superhydrophobic and superoleophilic surfaces:

The water contact angle (CA) θ was used to measure the wettability of a flat surface, which is depending on the solid-vapour, solid-liquid, and liquid-vapour surface tensions, and can be expressed by the Young's equation

$$\cos \theta = \frac{\gamma_{SV} - \gamma_{SL}}{\gamma_{LV}}$$

where γ_{SV} , γ_{SL} and γ_{LV} are the interfacial tensions between solid and vapour, solid and liquid, and liquid and vapour, respectively, as shown in Fig. 2. Depending on the value of the contact angle, surface properties are determined as hydrophilic, hydrophobic and superhydrophobic. If the water contact angle (θ) is less than 90° , the surface is described as hydrophilic, if θ is between 90° and 150° then hydrophobic and if θ is above 150° , the surface is described as superhydrophobic.

The wettability of solid surfaces depends upon the topography and the chemical composition of the surface.³⁷ Butterfly wings³⁸ and lotus leaves³⁹ are fine examples of natural hydrophobic materials. The artificial hydrophobic surfaces can be created by introducing roughness (micro or nanoscale asperities) and low surface energy materials.⁴⁰⁻⁴² For rough, hydrophobic surfaces, there are two possible states of wetting: (i) the droplet can skip between the peaks of roughness (the Wenzel state)⁴³ and in complete contact with the solid surfaces i.e. homogeneous wetting, as shown in Fig. 3a, (ii) the droplet can suspend on the top of the asperities (the Cassie-Baxter state)⁴⁴ and the air was trapped in between the

asperities i.e. heterogeneous wetting, as shown in Fig. 3b. The surface energy plays an important role in both the cases. The relationship of water contact angle on rough surface (θ_{rough}) and flat surface (θ_{flat}) for homogeneous and heterogeneous wettings are described by the Wenzel and the Cassie-Baxter equations, respectively. These two equations are listed as follows:

Wenzel's equation

$$\cos \theta_{rough} = r \cos \theta_{flat}$$

Cassie-Baxter's equation

$$\cos \theta_{rough} = \phi_s \cos \theta_{flat} - (1 - \phi_s)$$

where r is the roughness factor, defined as the ratio of the actual surface area to the geometrical one, and ϕ_s is the area fraction of the solid surface that contacts water. Both the theories pointed out that a rough surface is essential for enhancing hydrophobicity and they are commonly used to explain the wetting behaviour on rough hydrophobic surfaces.

Carbon as a superhydrophobic and superoleophilic material:

An ideal sorbent material must have high porosity, large specific surface area, high selectivity, chemical inertness and excellent recyclability. Micro porous polymers⁴⁵⁻⁴⁷ have been used as sorbent material, but they take long time for degradation so cost environmental and ecological risk. In addition, they have brittle mechanical properties and relatively long and complicate preparation method. Superhydrophobic carbon-based materials can be produced by various methods.⁴⁸ High surface area, low density, excellent flexibility, good chemical stability, environmental friendliness and large pore volume of carbon materials make them suitable candidates for water filtration, water/oil separation, oil spill cleanup, wastewater treatment, gas separation and purification.⁴⁹ Carbon aerogels, carbon nanotube forests, graphene foams or sponges, carbon coatings, activated carbon, porous carbon nanoparticles and carbon fibers have been widely used as sorbents owing to their excellent oil absorption capacity and reusability. The absorption capacity of the materials are defined as

$$\text{Absorption capacity} = \frac{m_a - m_d}{m_d}$$

where, m_a and m_d are the weights of the material after and before absorption, respectively.

Carbon nanotubes-based sorbent:

Carbon nanotubes have been demonstrated to have potential application in the fields of oil-water separation and gas adsorption, with a number of advantages, including stronger mechanical properties, rapid sorption rates, high sorbent capacity and engineered surface chemistry.⁵⁰⁻⁵⁷ Various techniques have been reported to synthesize carbon nanotubes such as arc discharge,⁵⁸ laser ablation,⁵⁹ pyrolysis,⁶⁰ electrochemical methods⁶¹ and chemical vapour deposition^{62,63} etc. Sun et al.⁶⁴ reported p-phenylenediamine modified carbon nanotubes (P-CNTs) synthesized by

diazotization reaction. The functionalization of CNTs by *p*-phenylenediamine was done to increase surface roughness and lower its surface free energy by the introduction of organic molecules. The P-CNTs showed rough and incompact morphology with high mesopore ratio, and the pore volume and mesopore volume were calculated to be 0.65 and 0.64 cm³ g⁻¹, respectively. Brunauer–Emmett–Teller (BET) surface area was measured to be 285 m² g⁻¹. The P-CNTs showed good hydrophobicity with water contact angle of 140.8°. The maximum absorption of the P-CNTs for oil and organic solvent was 3 to 12 times their own weight while repelling water completely. The absorbed oil and organic solvent can be recollected simply by heat treatment or solvent washing. The P-CNTs sorbent can be reused several times but the absorption capacity decreased a little after every use because of the residual oil and organic solvent which cannot be removed completely during heat treatment or solvent washing.

Gui et al. fabricated carbon nanotube sponge⁶⁵ and magnetic CNT sponge⁶⁶ by chemical vapour deposition (CVD) using ferrocene and dichlorobenzene. The CNT sponges showed highly interconnected, porous three-dimensional framework, as shown in Fig. 4a and b. The pore sizes of the sponges were ranged from several nanometres to a few micrometres. The sponges have excellent mechanical properties such as large strain deformation with almost full volume recovery and resistance to structural fatigue under cyclic stress conditions in oils, as shown in Fig. 4c and d. The sponge also exhibits excellent chemical stability in the air as well as oil and organic solvent with pH values ranging from 1-13. Under atmospheric conditions, the magnetic CNTs sponge can retain its hydrophobicity at least for one year. The CNT sponge and magnetic CNT sponge possessed hydrophobic properties with water contact angle of 156° and 140°, respectively. The density of carbon nanotube sponge and magnetic carbon nanotube sponge was measured to be 5-10 mg cm⁻³ and 15 mg cm⁻³, respectively. The absorption capacity of magnetic sponge and CNT sponge ranged from 49-56 and 80-180 times its own weight for different oils and organic solvents, respectively. The high absorption capacity of carbon nanotube sponge compared with magnetic carbon nanotube sponge was attributed to its lower density and better hydrophobicity. A spherical monolith of carbon nanotube sponge, when placed in an oil-water mixture, completely absorbed all oil and became a rectangular monolith, as shown in Fig. 4e. The sponge can be used more than 1000 times without significant change in its structure, water contact angle and absorption capacities.

Lee et al.⁶⁷ fabricated vertically-aligned CNT on stainless steel substrate by thermal chemical vapour deposition with a diffusion barrier of Al₂O₃ film. This stainless steel-CNT mess can be used as a filter for oil and organic solvent. This filter showed water contact angle of 150° and prevented 80% of water to pass through the mess. Heating the mess enhanced the flow rate of the viscous emulsion passing through the mess. Also, the water droplet size influenced the filtration and the mess was unable to prevent the pass of fine droplets. Gea et al.⁶⁸ demonstrated a magnetically superhydrophobic bulk material having absorption capacity of 0.71-1.15 times its own

weight. The bulk material was prepared by hot pressing method using PTFE, multiwall CNTs and iron oxide. The surface as well as interior of the bulk material was found superhydrophobic with water contact angle of 158°. The absorbed oil can be removed by burning in air while the bulk material is thermally stable. The absorption capacity of the bulk material only slightly decreased even after 10 oil removal cycles. Liu et al.⁶⁹ fabricated CNT foam with high mechanical strength and controlled shape by low temperature chemical fusion. The CNT foam exhibited highly entangled CNT well covered by disordered carbon species. The absorption capacity of the CNT foam was calculated to be 650 Kg m⁻³. Hashim et al.⁷⁰ synthesized 3D macroscale nanotube elastic solids using aerosol-assisted catalytic chemical vapour deposition via a boron doping strategy. The boron doping resulted in the formation of elbow junctions and nanotube covalent interconnections which enhanced the mechanical properties of the bulk material. Also, it provided high aspect ratio which enhanced the absorption capacity. The as-prepared sorbent has shown the absorption capacity of 22-180 (described as the ratio of the weight after and before absorption) for different oils and organic solvents.

There are several benefits of magnetic sorbents^{65, 68, 70} in the absorption of oil and organic solvents from water. After saturated absorption, the magnetic sorbent can be easily collected under manipulation by a magnetic apparatus. Moreover, the magnetic sorbent can be easily moved towards the polluted area with the help of an appropriate external magnetic field, thus it provides fast absorption of oils and organic solvents. In some applications where the accidental damage to the sorbent is unpreventable, all the broken parts of the magnetic sorbent can be collected in a controllable way more safely by a magnetic apparatus. Also, the magnetic sorbents can be easily kept in sight through magnetic tracking even with small fields.

The CNTs coated sponges have been widely used as a reusable oil sorbent scaffold in water, with high oil absorption capacity and good reusability.⁷¹⁻⁷³ Sponge is a three-dimensional porous polymer material which can absorb both oil and water, as shown in Fig. 5a. The CNTs on sponges altered its nature to only absorb oil while repel water completely, as shown in Fig. 5b. The coating creates micro and nano textured surface which provides superhydrophobic surfaces, as shown in Fig. 5c. Also, CNT coating significantly improved its thermal and mechanical stability. In some reports, several polymeric materials, such as PDMS and PVDF, have been used to not only improve the adhesion between CNT and sponge but also provide lower surface energy. The absorption capacity of CNT coated sponges ranged between 15-50 times their own weight and the absorbed oil can be reclaimed by mechanical squeezing^{71,72} and vacuum sucking⁷³.

Graphene-based sorbent:

Graphene-based materials have attracted significant attention in the field of oil spill cleanup because of their intrinsic hydrophobicity, high specific surface area along with excellent

chemical, thermal and mechanical stability.⁷⁴⁻⁷⁷ Graphene can be derived from various techniques such as mechanical exfoliation, chemical vapour deposition,⁷⁸ reduction of graphene oxide,⁷⁹ carbon dioxide reduction⁸⁰ and carbon nanotube slicing⁸¹ etc. Bi et al.⁸² reported spongy graphene absorbent with fast absorption rate of $0.57 \text{ g g}^{-1} \text{ s}^{-1}$ of dodecane and absorption capacity of 20-86 times its own weight. The spongy graphene having micro porous needle like structures was fabricated by chemical reduction of graphene oxide in suspension followed by shaping via molding. The work mentioned that it was difficult to completely remove all the functional groups but small amount of proper hydrophilic groups increased the interaction between polar solvents and graphene surfaces thus enhanced absorption capacity. The absorption capacity of thermally reduced graphene (TRG) fabricated by Iqbal et al.⁸³ depended on the bulk density, total pore volume and C/O ratio of TRG, which can be tuned by controlling the exfoliation condition. As the C/O ratio increases, the surface area and the cumulative pore volume increase resulting in better sorption capacity. The TRG samples with highest C/O ratio of 17:1 showed highest sorption capacity of $131\text{-}108 \text{ g g}^{-1}$. Wang et al.⁸⁴ proposed a green method for chemical reduction of graphene oxide using a range of natural phenolic acid. Among various natural phenolic acid, the best results were found in case of gallic acid in terms of low density, better mechanical properties and absorption capacity. Graphene reduced by natural phenolic acid can absorb not only oils with absorption capacity of 15-61 its own weight but also different kinds of dyes with absorption capacity of $115\text{-}1260 \text{ mg g}^{-1}$ sorbent.

Graphene aerogels, fabricated by different approaches such as solvent exchanging followed by freeze-drying,^{85,86} hydrothermal cross-linking and polymerization,^{87,88} freezing-drying,^{89,90} oil bath followed by a chemical reaction vessel and freezing-drying⁹¹ etc., have shown great potential in the field of oil spill cleanup due to their ultra-lightness, high compressibility, tremendous porosity and high specific surface area. Li et al.⁹² reported compressible and fire-resistant graphene aerogel produced by ethylenediamine and graphene oxide. The aerogel has a low density in the range of $4.4\text{-}7.9 \text{ mg cm}^{-3}$ and porosity up to 99.6% resulting in high absorption capacity up to 250 times its own weight for carbon tetrachloride. Also, the aerogel has shown faster absorption rate of $27 \text{ g g}^{-1} \text{ s}^{-1}$ as compared to pure graphene⁸² ($0.57 \text{ g g}^{-1} \text{ s}^{-1}$). The graphene aerogel can be reused by compression, combustion, distillation and squeezing with a little decrease in absorption capacity of 4% after ten cycles, 10% after five cycles, 7% after five cycles and 6% after five cycles, respectively. Zhao et al.⁹³ reported ultra-light, three dimensional, nitrogen doped graphene framework produced by graphite oxide and pyrrole using the hydrothermal method followed by freezing drying and annealing. The electron rich N atoms present in the pyrrole structure facilitated its attachment to the galleries and surface of GO sheets through hydrogen bonding or $\pi\text{-}\pi$ interaction and also provided fire resistance properties, as shown in Fig. 6a. It can sustain up to $1200 \text{ }^\circ\text{C}$ in N_2 and $600 \text{ }^\circ\text{C}$ in air. The graphene aerogel has

shown self-assembled, porous, interconnected, three-dimensional framework, as shown in Fig. 6b, with an ultra-light density of $2.1\pm 0.3 \text{ mg cm}^{-3}$, which is comparable to the density of air (1.2 mg cm^{-3}) at room temperature, as shown in Fig. 6c. The pyrrole also prevented re-stacking of reduced GO sheets, resulting in the formation of high porous volume of graphene framework. The graphene framework has excellent mechanical and thermal stability as well as high absorption rate of $41.7 \text{ g g}^{-1} \text{ s}^{-1}$ which is the highest among the previous reported pure graphene⁸² and graphene aerogel⁹²; in addition, it has high absorption capacity of 200-600 times its own weight for different oils and organic solvents, as shown in Fig. 6d.

Gao et al.⁹⁴ fabricated reduced graphene oxide foam using three different freezing-drying methods i.e. unidirectional, non-directional and air freezing-drying method. The graphene oxide concentration and different freezing-drying methods affected the pore size of the material. The largest and most ordered pores were found in case of unidirectional freezing-drying method. The reduced graphene oxide foam has absorption capacity of 90-123 times its own weight but the absorption capacity decreased by one third in second cycle and after second cycle it remained constant. Also, the absorption capacity varied with temperature and found maximum at $15 \text{ }^\circ\text{C}$. Covalently intercalated graphene oxide, prepared by Liu et al.⁹⁵ using graphene oxide and octavinyl polyhedral oligomeric silsesquioxane, can effectively separate two miscible solvents according to their solvent density. But it can only separate the mixer of two solvent if one solvent has density higher than water and the other lower than water. It cannot separate the solvents have densities both higher or lower than water. The material is superhydrophobic and formed a stable dispersion in solvents except water so it can easily push out water from oil and organic solvents.

The rapid evolution of the gaseous species (e.g. H_2O and CO_2) formed during chemical reduction of graphene oxide can trigger the formation of porous structure. The compact layered graphene oxide structures as "dough" were very important for the rapid evolution of the gaseous species. The crosslinked structures of pore walls can prevent the restacking of graphene sheets without the help of any spacers or templates resulting in open porous network. Based on this idea, Niu et al.⁹⁶ reported autoclave leavening process to synthesize porous reduced graphene oxide foam. The absorption capacity of reduced graphene foam was measured to be 26-37 times its own weight. Yang et al.⁹⁷ also synthesized freestanding reduced graphene oxide film by adjusting the heating rate to control the macroporosity of the film. The work concluded that the higher heating rate can rapidly generate gases resulting in the significant volume expansion. The film can absorb 8-45 times its own weight depending on the density of the oil and organic solvent and can be reused by heating under vacuum or mechanical squeezing.

The intrinsically hydrophobic graphene coated porous materials such as sponges, fibers and cottons prepared by dip coating,^{32,98-104} hydrothermal,¹⁰⁵ and grafting polymerization¹⁰⁶ have been reported as oil absorbent. The low densities, good mechanical properties, cost effectiveness and high absorption

capacities of porous materials make them very useful in this field. However, these commercially available porous materials absorb both oil and water so further modification is required to switch their wettability from superhydrophilic to superhydrophobic while maintain their capability of absorbing oil and organic solvent.

Our group⁹⁸ reported graphene nanosheets coated melamine sponge, as shown in Fig. 7a, which performed superhydrophobic and superoleophilic properties showing high absorption capacity of 54-165 times its own weight for different oils and organic solvents, as shown in Fig. 7b. As shown in figure 7c, the water contact angle on graphene nanosheets was measured to be 132° while it was found 160° on graphene coated sponges with a graphene loading of 7.3%. The smooth sponge skeletons, as shown in Fig. 7d, turned to mono-roughened surface composed of the micro-porous structure after coating with graphene nanosheets and PDMS, respectively, as shown in Fig. 7e and f. TEM image of graphene nanosheets confirmed the planar structure with wrinkling surfaces and folding edges, as shown in Fig. 7g. The work reported that the unsaturated graphene loading (less than 5.1%) cannot alter its wettability while oversaturated loading (more than 7.3%) cannot further improve its superhydrophobicity (water contact angle 160°) and may block the sponge pores. The absorption capacity of the graphene coated sponges for oils decreased to less than 20 times and 18 times the weight of the previously used sponge after first and second cycle, respectively, owing to residual oil which cannot be extracted by mechanical squeezing while it remained almost the same for organic solvents till five cycles, as shown in 7h and i, respectively.

Liu et al.⁹⁹ prepared oil absorbent by coating polyurethane sponge with graphene oxide and reduced graphene oxide. The absorption capacity of the reduced graphene oxide coated sponges (80-160 times its own weight) was found better than graphene oxide coated sponges (70-140 times its own weight) because of its higher porosity and presence of fewer oleophilic polar groups on its surface. Moreover, the graphene oxide coated sponges have shown better reusability compared to our group⁹⁸ and did not change even after 50 cycles.

Sun et al.¹⁰⁰ fabricated reduced graphene oxide coated cottons with absorption capacity of 11-25 times its own weight. Ge et al.¹⁰⁴ reported graphene coated cotton with absorption capacity of 30-50 times its own weight. The absorption capacities of cotton-based absorbents were found much lower compared to graphene coated sponges^{98,99}. The absorption capacity of the absorbent strongly depends on the porosity, density and hydrophobicity of the material. The huge difference in the absorption capacity of the graphene coated sponge^{98,99} and graphene coated cotton^{100,104} is due to the differences in these properties. It is known that the porosity of cotton is much lower than that of sponge. This is why the absorption capacities of graphene coated sponges are much higher than graphene coated cotton.

Sun et al.¹⁰² also synthesized three dimensional superwetting graphene mesh film on stainless-steel grids. It was found that the water droplet has taken spherical shape with water

contact angle 152° and did not slide even if the film was tilted vertically or kept upside down. Owing to this unique property, the film can be used to remove small amount of water from oil-water mixture.

For better adhesion between graphene and sponges or cotton, the low surface energy materials like PDMS have been used to cement the graphene with the porous materials.^{98,99,102} Li et al.¹⁰³ coated polyurethane sponge with 11.96% loading of KH-570 modified graphene to increase its roughness, which have absorption capacity of 39 times its own weight. The as-prepared sponges have good recyclability because the absorption capacity did not change even after 120 cycles. A water-oil separation material with separation efficiency of more than 90% was fabricated by Wu et al.³². The sponge was prepared by the self-assembly of graphene sheets on a 3D polymer skeleton. The as-prepared sponges have a crinkled and rough textured morphology and excellent mechanical properties because of flexible graphene sheets. Superhydrophobic foam prepared by the grafting polymerization method was first reported by Liu et al.¹⁰⁶. They synthesized the superhydrophobic foam by directly grafting primary amine groups functionalized graphene oxide onto polyurethane sponges with nitrile group using in situ amidation. Compared with the blank foams, the as-modified foam has shown enhanced absorption capacity for solvents due to better interaction force between modified foam and solvents. The absorption capacity of the modified foam was measured to be 26-41 times its own weight for different oils and organic solvents.

Carbon aerogels:

To date, pyrolysis of biomass is considered to be the simplest approach to produce carbon materials as it is cheap, sustainable, green preparation process and the as-prepared materials are biocompatible and biodegradable. Various kinds of biomass such as raw cotton,^{107,108} winter melon,¹⁰⁹ kapok wadding materials,¹¹⁰ waster paper¹¹¹ and bacterial cellulose pellicles¹¹² have been used to prepare carbon aerogels. During the pyrolysis process of biomass, the hydrophilic functional groups such as C=O, C-O, C-H, and O-H were removed while keeping its oleophilic properties. These carbon aerogels have porous and interconnected three dimensional networks with good mechanical and fire resistant properties. Also, it is reported that the pyrolysis temperature has played an important role in achieving hydrophobic surfaces.^{107,111} Carbon aerogel prepared by the pyrolysis of winter melon have shown density of 48 mg cm⁻³ and absorption capacity of 16-50 times its own weight¹⁰⁹. Carbon aerogels prepared by Huang et al.¹¹⁰ using kapok wedding materials have shown ultralow density of ≈2.4 mg cm⁻³ which is comparable to previously reported graphene framework⁹³. The absorption capacity of carbon aerogel derived from kapok wedding material was measured to be 87-273 times its own weight. Wu et al.¹¹² have synthesized carbon aerogel by destroying the crystalline structure of bacterial cellulose pellicles to form amorphous carbon aerogel through freezing-drying process followed by

pyrolysis, as shown in Fig. 8a and b. Also, the pyrolysis temperature has an effect on water contact angle which increases with increases temperature, as shown in Fig. 8c. This kind of carbon aerogel has high absorption capacity of 106-312 times its own weight and can be regenerated by distillation and direct combustion in air. The aerogel has shown fire-resistance property, as shown in Fig. 8d, and it can sustain more than 90% volume reduction once subjected to compression and almost recover its original volume when released, thus showed good mechanical properties. There is a significant difference of absorption capacities between the aerogels prepared by three different raw materials i.e. winter melon, kapok wedding material and bacterial cellulose pellicles. The absorption capacity of the materials is highly affected by the bulk density of the materials. Less dense materials show high absorption capacity because they provide more internal free volume for absorption. The density of winter melon aerogel is remarkably high compared with kapok wedding aerogel and bacterial cellulose pellicles aerogel. This is why the absorption capacity of winter melon aerogel was much lower than that of kapok wedding aerogel and bacterial cellulose pellicles aerogel.

Men et al.¹¹³ reported that the sugar-based molecules and polysaccharide biomass can be converted into porous functional carbon absorbent by ionic liquid or poly(ionic liquid) at low temperature of 400 °C under nitrogen atmosphere. The ionic liquid or poly(ionic liquid) acted as activation agent and effectively induced carbonization and pore generation, resulting in the formation of porous carbon absorbent.

Besides pyrolysis of biomass, other techniques and materials have also been reported to synthesized carbon aerogels. Wang et al.¹¹⁴ prepared hydrophobic carbon aerogel by dissolution, gelation, regeneration, freeze-drying and carbonization of cellulose. The as-prepared carbon aerogel have shown high porosity (98%) and fast absorption to organic dyes and heavy ions with absorption capacities of different dyes in the range from 195 to 1947 mg g⁻¹. Moreover, the carbon aerogel has shown fire resistant property and good reusability since the saturated absorption capacity did not change after five cycles. Wu et al.¹¹⁵ produced carbon nanofibers aerogel using template directed hydrothermal carbonization method followed by freeze drying and pyrolysis, which can sustain over a wide temperature range from liquid nitrogen to 400 °C. The self-assembled, interconnected, three-dimensional structure of carbon aerogel possesses both micropores and macropores and has shown porosity of more than 99%. The absorption capacity of carbon nanofibers aerogel was 139 times its own weight and it did not change over ten absorption-reclamation cycles. Nitrogen rich carbon aerogel fabricated by Yang et al.¹¹⁶ can absorb micrometre sized oil droplet with high efficiency which is an important feature in marine oil-spill recovery as spilled oils often breaks into many micrometre sized droplets by waves and wind.

Graphene and CNTs aerogels have shown good absorption capacity and reusability because of their low density, high aspect ratio, good elasticity and excellent mechanical properties. As compared with others, the absorption capacity

can be enhanced by taking the advantage of both CNTs and graphene by preparing the hybrid structure of graphene and CNTs. CNTs can be used to increase the surface roughness of graphene resulting in better hydrophobicity and enhanced absorption capacity. Based on this idea, different techniques such as ultrafast microwave irradiation (MWI)-mediated approach,¹¹⁷ two-step chemical vapor deposition,¹¹⁸ thermal process followed by freezing drying¹¹⁹ and freezing drying followed by chemical reduction¹²⁰ have been reported to fabricate graphene-CNTs hybrid structure. Hu et al.¹¹⁷ prepared ultra-light graphene aerogel (ULGA) and graphene aerogel-CNTs (GA/CNTs) hybrid and concluded that the water contact angle of ULGA without containing CNTs is 100° which increased with the incorporation of CNTs, and it was found that with 14 wt.% CNTs, the GA/CNTs showed a water contact angle of 110° and it increased with increasing the amount of CNTs until 37 wt.% where the GA/CNTs performed superhydrophobicity. The improved hydrophobicity can be attributed to the nano-roughness created by the CNTs on the smooth walls of ULGA and the air trapped in the nanoscopic voids in the CNT forest. Dong et al.¹¹⁸ used two steps CVD to prepare highly flexible superhydrophobic 3D graphene-CNT hybrid foam with water contact angle of 152.3° and absorption capacity of 80-130 times its own weight. For a comparative study, Dong et al. also prepared 2D and 3D graphene and the water contact angle on 2D and 3D graphene were found 89.4° and 108.5°. As compared with 2D graphene, the air trapped in the microscopic structure of 3D graphene is responsible for the improved hydrophobicity while in the case of 3D graphene-CNT hybrid foam, the superhydrophobicity was found because of the nano-roughness created by CNTs and the air trapped in both macroscopic voids of 3D graphene as well as nanoscopic voids of CNTs.

To overcome the two-step process proposed by Dong et al.,¹¹⁸ Kabiri et al.¹¹⁹ suggested a one step process to fabricate graphene-CNTs aerogel without using harsh chemicals. The graphene oxide was reduced using the iron (Fe) nanoparticles by heating which were mixed with the acid treated CNTs to fabricate the aerogel. The CNTs acted as a spacer between graphene sheets thus resulting in a highly porous structure of graphene-CNTs aerogel. One gram of aerogel can absorb 28 L of oil and the absorption capacity was found 21-35 times its own weight for different oils and organic solvents. Sun et al.¹²⁰ used giant graphene oxide and CNTs to prepare ultra-flyweight aerogels (UFAs), as shown in Fig. 9a, by freezing drying of aqueous solution of CNTs and giant graphene oxide followed by chemical reduction of giant graphene oxide with hydrazine vapour. The as-prepared UFAs have shown interconnected, porous three dimensional graphene structure covered with entangled, spaghetti-like CNTs network in form of overlapping, twisting and enwrapping, as shown in Fig. 9 b-d. The UFAs have shown low density (0.16-22.4 mg cm⁻³), excellent porosity (≈99.9%) and ultra-high absorption capacity of 215-913 times its own weight for different oils and organic solvents. Moreover, the UFAs have shown fast absorption, as shown in Fig. 9e, elasticity-responsive conductivity and temperature-invariant super recyclability. UFAs can also absorb solids by

converting into phase change energy storage materials through melting infiltration.

Graphite:

Exfoliated graphite has also been a promising candidate in oil spill recovery as it can quickly absorb heavy oil floating on water.¹²¹⁻¹²³ Exfoliated graphite can be prepared by rapid decomposition of natural graphite at high temperature ($\approx 1000-1200$ °C). When natural graphite was heated at high temperature, it generated various gaseous compounds which helped in the exfoliation of natural graphite resulting in the formation of porous structure. The exfoliation of natural graphite can be prepared by various methods such as microwave irradiation method¹²⁴ and chemical intercalation followed by thermal treatment^{125,126}. One gram of exfoliated graphite absorbent, prepared by Bayat et al.¹²⁵ using a mixture of sulfuric acid and nitric acids, followed by thermal shock of graphite intercalated compound, can absorb 70-87 grams of different oils. Hristea et al.¹²⁶ also prepared exfoliated graphite absorbent through thermal expansion of H₂SO₄-graphite intercalated compound. KMnO₄ or FeCl₃ were used as an oxidizing agent but the KMnO₄ treated compounds have shown better specific volume expansion compared with FeCl₃ treated compounds due to its higher degree of graphite oxidation. In spite of better specific expansion volume shown by KMnO₄, the FeCl₃ treatment is considered to be most desirable because of its slightly exothermic reaction and easier filtration procedure. Also, different pore volumes and surface areas were shown by different molar ratios of H₂SO₄:HNO₃ reagents, which resulted in different absorption capacities. The absorption capacity was measured to be 2.4-9.7 L per 100 g of absorbent.

Toyoda et al.¹²⁷ tested the absorption capacity of commercially available exfoliated graphite prepared by industrial process in terms of temperature and compression. Different bulk densities of exfoliated graphite were prepared by compressing the bulk graphite, which resulted in different pore volumes thus, different absorption capacities. It is found that the absorption capacity decreased with decreasing temperature which is attributed to the increase in viscosity of oil with decreasing temperature. The maximum absorption capacity was measured to be 80-90 gram of oil per gram of absorbent with recovery ratio of 60-80% through simple compression or suction filtration. Graphite/isobutylene-isoprene rubber cryogels, prepared by Hu et al.¹²⁸ through freeze-thaw or cryogelation method using sulfur monochloride as the crosslinker, have shown an interconnected porous network with fractured surfaces. The reaction temperature and the amount of graphite were adjusted to obtain better hydrophobicity and absorption capacity. The nonporous structures with compact surfaces were found at the temperature above 0 °C because the temperature was not low enough to freeze the benzene and thus form pores. The porous structures were found below 0 °C but the pore volume decreased with decreasing temperature because of higher nucleation rate. It was also concluded that the high amount of

graphite can lead to low absorption capacity, thus appropriate amount of graphite is required for better results. One gram of cryogels, prepared at -15 °C with 2 wt./wt.% graphite, can absorb 17.6-23.4 gram of different oils and lubricants with faster absorption rates.

Wang et al.¹²⁹ prepared modified expanded graphite (MEG) nanomaterials by strong acid treatment using H₂O₂ as the oxidant and concentrated H₂SO₄ as the intercalator. Field emission scanning electron microscopy analysis revealed that the MEG has worm-like morphologies, as shown in Fig. 10a, with three different kinds of pores; (i) many V-type pores (dimension from several dozens of μm to several hundreds of μm) on the surface (ii) willow leaf type pores (dimension from several μm to several dozens of μm), as shown in Fig. 10b and (iii) pores formed by up and down of the pore walls, as shown in Fig. 10c. The V-type pore and willow leaf type pores provided the internal storage for oil absorption. The as-prepared MEG can absorb different kinds of industrial oil with absorption capacities ranging from 43.25 to 84.68 g g⁻¹ of MEG for expanded volume of 100-320 mL g⁻¹, as shown in Fig. 10d. In addition, it was also found that the absorption capacity increases with increasing viscosity since the high viscosity of the oil provides higher glutinosity.

Other carbon forms:

Porous carbon nanoparticles, prepared by Dai et al.,¹³⁰ have also been reported as superhydrophobic material with a water contact angle of 150°. These porous carbon nanoparticles were prepared by glow discharge of hydrocarbon plasma without a catalyst at room temperature by using C₂H₂ and a gas mixture of C₂H₂ and CF₄. The low surface energy resulted in better hydrophobicity which is attributed to the fluorine content present in the porous carbon nanoparticles. Also, the CF₄/C₂H₂ ratio and deposition pressure were crucial for surface morphology. The as-prepared porous carbon nanoparticles can separate oil/water mixture as well as the mixtures of liquids with different surface tension levels. Gao et al.¹³¹ fabricated carbon soot sponges which have shown good absorption capacity and recyclability for different oils and organic solvents. The carbon soot was prepared by the combustion flame method using ethylene and oxygen as precursors with a flow ratio of 5:3 and then carbon soot was loaded on melamine sponges by simple dip coating, as shown in Fig. 11a. The amorphous carbon structures with size ranges of 5-50 nm have shown randomly entangled and rippled graphitic striations in the inner cores and on the outer layers, respectively. The uniform coating of carbon soot on the sponge resulted in the nanoscale porous surface with hierarchical porous structure, as shown in Fig. 11b-d, which facilitate the successful absorption of oil and organic solvent while repelling water completely, as shown in Fig. 11e. The water contact angles on the carbon soot surface and carbon soot sponges (loaded with ≈ 9 wt% carbon soot) were measured to be 140° and 144°, respectively. The absorption capacity and hydrophobicity were highly affected by the loading percentage of carbon soot, as shown in Fig. 11f. The

absorption capacity did not change till 10 cycles but after 10 cycles, it became 94% of the initial absorption capacity. The carbon soot sponges have shown the absorption capacity of 25-80 times its own weight for different oil and organic solvents, as shown in Fig. 11g. The as-prepared carbon soot sponges were quite economical compared with other carbon forms.

Xiao et al.¹³² used coal liquefaction residue to synthesize carbon nanofibers/carbon foam composite with absorption capacity of 15-28 times its own weight for different oils and organic solvents. First, the carbon foam was prepared by the template synthesis of carbon and then catalytic chemical vapour deposition was used to grow carbon nanofibers on carbon foam substrates. The iron species present in the coal liquefaction residue were acted as a catalyst. The entangled carbon nanofibers covered the entire surface of carbon foam thus enhanced surface roughness resulting in better hydrophobicity (water contact angle $\approx 140^\circ$). Cortese et al.¹³³ roughened the smooth surface of cotton textile, using oxygen plasma pre-treatment followed by the coating of diamond-like materials through plasma enhanced chemical vapour deposition, to fabricate superhydrophobic cotton fabrics. The surface morphology of the cotton fabrics was highly affected by the plasma pre-treatment time as well as content of methane and hydrogen in the coating process. Longer oxygen plasma pre-treatment process increased the etching of the polymers and cellulose containing oxygen groups in the cotton textile which resulted in the formation of the nanometre-scale rough surface available for the diamond-like coating. This effect can be seen while measuring the water contact angle on oxygen plasma treated surfaces ($169.3^\circ \pm 2.2^\circ$) and untreated surfaces ($143^\circ \pm 2^\circ$). The absorption capacity for this kind of cotton fabric was measured to be 55-94 times its own weight and it did not change even after 5 cycles of oil-water separation.

Shi et al.¹³⁴ fabricated carbonaceous nanoparticles (CNPs) modified polyurethane (PU) foam using ultrasonication technique. This work concluded that the jets and shock waves, originated through the ultrasonication, softened or even partially melted the PU foam as well as pushed the carbonaceous nanoparticle towards the PU foam which resulted in the successful attachment of carbonaceous nanoparticles on the PU foam. The effect of nanoparticle dimension was also investigated and it was concluded that the nanoparticle anchored foam has rougher surface compared with CNT or GO anchored foam because the nanoparticles gained high kinetic energy because of its size and shape. The CNPs-PU foam can sustain 500 cycles of compressing at 80% compressing strain without any plastic deformation. The CNPs-PU has shown water contact angle of 127.6° and it can absorb different organic solvent to 50-121 times its own weight. A superhydrophobic and superoleophilic disc made from hollow carbon bead was fabricated by Zeng et al.¹³⁵ using a simple phase inversion method and subsequent carbonisation of polysulfone bead. It was found that the pore-forming additive tetraethyl orthosilicate was responsible for the big hollow pores which were formed in the polymer during the phase

inversion process. The silica powder also supported polymer beads during carbonisation because without silica powder the beads collapsed. The percentage of silica also influenced absorption capacity as it acted as a template and provided big hollow sphere. The carbon beads can absorb different oils and organic solvents to 50-55% of their own weight and it remained same till five absorption/heat treatment cycles.

Briefly, the best performances of different carbon-based absorbents have been summarized in Table 1.

Conclusions

Carbon-based sorbents have shown great capabilities in oil-spill cleanup operations owing to their superior properties. Moreover, they are biodegradable and chemically inert which make them superior over polymer-based sorbents. Different forms of carbon-based sorbents such as carbon aerogels, carbon nanotube forests, graphene foams or sponges, carbon coatings, activated carbon, porous carbon nanoparticles and carbon fibers have been widely used as sorbents because of their excellent oil absorption capacity and reusability. Coating of CNTs, graphene, graphite or hybrid of these on polymer sponge has also been widely used to produce superhydrophobic and superoleophilic materials; as a result, altered its intrinsic nature to only absorb oil while repel water completely. Also, these carbon materials significantly improved its thermal and mechanical stability. The pyrolysis of biomass has also been used to produce carbon aerogel sorbents as it is a cheap, sustainable, chemical free green preparation process. CNTs-graphene hybrid aerogel have also been reported in which CNTs were used to increase the surface roughness of graphene resulting in better hydrophobicity and enhanced absorption capacity. The exfoliated graphite sorbents can be prepared by the rapid decomposition of natural graphite at high temperature which generates various gaseous compounds which helped in the exfoliation of natural graphite resulting in the formation of porous structure. These carbon-based sorbents have shown a wide range of absorption capacity from 3 to 913 times their own weight. Some sorbents can follow the continuous absorption/removal process through the vacuum pumping process. Carbon nanofibers/carbon foam composite, carbon soot sponge carbonaceous nanoparticles modified polyurethane foam and hollow carbon beads have also been reported for the water-oil separation.

Acknowledgements

The authors would like to thank Ministry of Science and Technology, Taiwan, for the financial support through the project of MOST 104-2221-E-007-029-MY3.

Notes and references

- 1 C. Campagna, F. T. Short, B. A. Polidoro, R. McManus, B. B. Collette, N. J. Pilcher, Y. Sadovy de Mitcheson, S. N. Stuart and K. E. Carpenter, *BioScience*, 2011, **61**, 393-397.
- 2 <http://www.appledaily.com.tw/realtimenews/article/like/20150715/648694/>, (accessed August 2015)
- 3 P. F. Kingston, *Spill Science & Technology Bulletin*, 2002, **7**, 53-61.
- 4 R. Edwards and I. White, *International Oil Spill Conference Proceedings*, 1999, **1999**, 97-102.
- 5 V. Broje and A. A. Keller, *Environmental Science & Technology*, 2006, **40**, 7914-7918.
- 6 M. A. Zahed, H. A. Aziz, M. H. Isa, L. Mohajeri and S. Mohajeri, *Bioresource Technology*, 2010, **101**, 9455-9460.
- 7 I. Buist, S. Potter, T. Nedwed and J. Mullin, *Cold Regions Science and Technology*, 2011, **67**, 3-23.
- 8 E. B. Kujawinski, M. C. Kido Soule, D. L. Valentine, A. K. Boysen, K. Longnecker and M. C. Redmond, *Environmental Science & Technology*, 2011, **45**, 1298-1306.
- 9 S.-Z. Yang, H.-J. Jin, Z. Wei, R.-X. He, Y.-J. Ji, X.-M. Li and S.-P. Yu, *Pedosphere*, 2009, **19**, 371-381.
- 10 R. Margesin and F. Schinner, *Appl Microbiol Biotechnol*, 2001, **56**, 650-663.
- 11 R. P. Swannell, K. Lee and M. McDonagh, *Microbiological Reviews*, 1996, **60**, 342-365.
- 12 L. Feng, Z. Zhang, Z. Mai, Y. Ma, B. Liu, L. Jiang and D. Zhu, *Angewandte Chemie*, 2004, **116**, 2046-2048.
- 13 H. Li, J. Wang, L. Yang and Y. Song, *Advanced Functional Materials*, 2008, **18**, 3258-3264.
- 14 T. R. Annunziado, T. H. D. Sydenstricker and S. C. Amico, *Marine Pollution Bulletin*, 2005, **50**, 1340-1346.
- 15 A. Bayat, S. F. Aghamiri, A. Moheb and G. R. Vakili-Nezhaad, *Chemical Engineering & Technology*, 2005, **28**, 1525-1528.
- 16 J. Xie, W. Meng, D. Wu, Z. Zhang and H. Kong, *Journal of Hazardous Materials*, 2012, **231-232**, 57-63.
- 17 J. Rulon E and D. Robert H, in *Contact Angle, Wettability, and Adhesion*, AMERICAN CHEMICAL SOCIETY, 1964, vol. 43, ch. 7, pp. 112-135.
- 18 T. Onda, S. Shibuichi, N. Satoh and K. Tsujii, *Langmuir*, 1996, **12**, 2125-2127.
- 19 J. Yuan, X. Liu, O. Akbulut, J. Hu, S. L. Suib, J. Kong and F. Stellacci, *Nat Nano*, 2008, **3**, 332-336.
- 20 J. Wu, N. Wang, L. Wang, H. Dong, Y. Zhao and L. Jiang, *ACS Applied Materials & Interfaces*, 2012, **4**, 3207-3212.
- 21 A. Walcarius and L. Mercier, *Journal of Materials Chemistry*, 2010, **20**, 4478-4511.
- 22 A. M. Atta, R. A. M. El-Ghazawy, R. K. Farag and A.-A. A. Abdel-Azim, *Reactive and Functional Polymers*, 2006, **66**, 931-943.
- 23 G.-R. Shan, P.-Y. Xu, Z.-X. Weng and Z.-M. Huang, *Journal of Applied Polymer Science*, 2003, **90**, 3945-3950.
- 24 X.-M. Zhou and C.-Z. Chuai, *Journal of Applied Polymer Science*, 2010, **115**, 3321-3325.
- 25 V. Janout, S. B. Myers, R. A. Register and S. L. Regen, *Journal of the American Chemical Society*, 2007, **129**, 5756-5759.
- 26 M. Inagaki, A. Kawahara and H. Konno, *Carbon*, 2002, **40**, 105-111.
- 27 T. Ono, T. Sugimoto, S. Shinkai and K. Sada, *Nat Mater*, 2007, **6**, 429-433.
- 28 T. Ono, T. Sugimoto, S. Shinkai and K. Sada, *Advanced Functional Materials*, 2008, **18**, 3936-3940.
- 29 Y. Chu and Q. Pan, *ACS Applied Materials & Interfaces*, 2012, **4**, 2420-2425.
- 30 S. Tao, Y. Wang and Y. An, *Journal of Materials Chemistry*, 2011, **21**, 11901-11907.
- 31 A. Sayari, S. Hamoudi and Y. Yang, *Chemistry of Materials*, 2005, **17**, 212-216.
- 32 C. Wu, X. Huang, X. Wu, R. Qian and P. Jiang, *Advanced Materials*, 2013, **25**, 5658-5662.
- 33 M. Inagaki, K. Shibata, S. Setou, M. Toyoda and J.-i. Aizawa, *Desalination*, 2000, **128**, 219-222.
- 34 S. Nardecchia, D. Carriazo, M. L. Ferrer, M. C. Gutierrez and F. del Monte, *Chemical Society Reviews*, 2013, **42**, 794-830.
- 35 G. Tao, L. Zhang, Z. Hua, Y. Chen, L. Guo, J. Zhang, Z. Shu, J. Gao, H. Chen, W. Wu, Z. Liu and J. Shi, *Carbon*, 2014, **66**, 547-559.
- 36 H. Sun, A. Li, Z. Zhu, W. Liang, X. Zhao, P. La and W. Deng, *ChemSusChem*, 2013, **6**, 1057-1062.
- 37 N. J. Shirlcliffe, G. McHale, S. Atherton and M. I. Newton, *Advances in Colloid and Interface Science*, 2010, **161**, 124-138.
- 38 W. Barthlott and C. Neinhuis, *Planta*, 1997, **202**, 1-8.
- 39 Y. Fang, G. Sun, T. Wang, Q. Cong and L. Ren, *CHINESE SCI BULL*, 2007, **52**, 711-716.
- 40 M. Ma and R. M. Hill, *Current Opinion in Colloid & Interface Science*, 2006, **11**, 193-202.
- 41 L. Cao, H.-H. Hu and D. Gao, *Langmuir*, 2007, **23**, 4310-4314.
- 42 X.-M. Li, D. Reinhoudt and M. Crego-Calama, *Chemical Society Reviews*, 2007, **36**, 1350-1368.
- 43 R. N. Wenzel, *Industrial & Engineering Chemistry*, 1936, **28**, 988-994.
- 44 A. B. D. Cassie and S. Baxter, *Transactions of the Faraday Society*, 1944, **40**, 546-551.
- 45 A. Li, H.-X. Sun, D.-Z. Tan, W.-J. Fan, S.-H. Wen, X.-J. Qing, G.-X. Li, S.-Y. Li and W.-Q. Deng, *Energy & Environmental Science*, 2011, **4**, 2062-2065.
- 46 A. M. Atta, S. H. El-Hamouly, A. M. AlSabagh and M. M. Gabr, *Journal of Applied Polymer Science*, 2007, **105**, 2113-2120.
- 47 R. K. Farag and S. M. El-Saeed, *Journal of Applied Polymer Science*, 2008, **109**, 3704-3713.
- 48 M. Long-Yue and P. Soo-Jin, *Carbon letters*, 2014, **15**, 89-104.
- 49 Z. Xue, Y. Cao, N. Liu, L. Feng and L. Jiang, *Journal of Materials Chemistry A*, 2014, **2**, 2445-2460.
- 50 X. Peng, Y. Li, Z. Luan, Z. Di, H. Wang, B. Tian and Z. Jia, *Chemical Physics Letters*, 2003, **376**, 154-158.
- 51 Q. Liao, J. Sun and L. Gao, *Colloids and Surfaces A: Physicochemical and Engineering Aspects*, 2008, **312**, 160-165.
- 52 X. Zhu, Z. Zhang, G. Ren, J. Yang, K. Wang, X. Xu, X. Men and X. Zhou, *Journal of Materials Chemistry*, 2012, **22**, 20146-20148.
- 53 Y. Jin, S. C. Hawkins, C. P. Huynh and S. Su, *Energy & Environmental Science*, 2013, **6**, 2591-2596.
- 54 Y.-H. Li, S. Wang, Z. Luan, J. Ding, C. Xu and D. Wu, *Carbon*, 2003, **41**, 1057-1062.
- 55 B. Pan and B. Xing, *Environmental Science & Technology*, 2008, **42**, 9005-9013.
- 56 M. S. Mauter and M. Elimelech, *Environmental Science & Technology*, 2008, **42**, 5843-5859.
- 57 S. Maphutha, K. Moothi, M. Meyyappan and S. E. Iyuke, *Sci. Rep.*, 2013, **3**.
- 58 T. W. Ebbesen and P. M. Ajayan, *Nature*, 1992, **358**, 220-222.

- 59 T. Guo, P. Nikolaev, A. G. Rinzier, D. Tomanek, D. T. Colbert and R. E. Smalley, *The Journal of Physical Chemistry*, 1995, **99**, 10694-10697.
- 60 T. Abdel-Fattah, E. J. Siochi and R. E. Crooks, *Fullerenes, Nanotubes and Carbon Nanostructures*, 2006, **14**, 585-594.
- 61 D. Zhou, E. V. Anoshkina, L. Chow and G. Chai, *Carbon*, 2006, **44**, 1013-1016.
- 62 N. H. Tai, H. M. Chen, Y. J. Chen, P. Y. Hsieh, J. R. Liang and T. W. Chou, *Composites Science and Technology*, 2012, **72**, 1855-1862.
- 63 C. Chien-Chao, T. Tsung-Yen and T. Nyan-Hwa, *Nanotechnology*, 2006, **17**, 2840-2844.
- 64 H. Sun, P. La, Z. Zhu, W. Liang, B. Yang, X. Zhao, C. Pei and A. Li, *J Mater Sci*, 2014, **49**, 6855-6861.
- 65 X. Gui, Z. Zeng, Z. Lin, Q. Gan, R. Xiang, Y. Zhu, A. Cao and Z. Tang, *ACS Applied Materials & Interfaces*, 2013, **5**, 5845-5850.
- 66 X. Gui, J. Wei, K. Wang, A. Cao, H. Zhu, Y. Jia, Q. Shu and D. Wu, *Advanced Materials*, 2010, **22**, 617-621.
- 67 C. H. Lee, N. Johnson, J. Drelich and Y. K. Yap, *Carbon*, 2011, **49**, 669-676.
- 68 B. Ge, Z. Zhang, X. Zhu, G. Ren, X. Men and X. Zhou, *Colloids and Surfaces A: Physicochemical and Engineering Aspects*, 2013, **429**, 129-133.
- 69 Y. Liu, H. Ba, D.-L. Nguyen, O. Ersen, T. Romero, S. Zafeiratos, D. Begin, I. Janowska and C. Pham-Huu, *Journal of Materials Chemistry A*, 2013, **1**, 9508-9516.
- 70 D. P. Hashim, N. T. Narayanan, J. M. Romo-Herrera, D. A. Cullen, M. G. Hahm, P. Lezzi, J. R. Suttle, D. Kelkhoff, E. Muñoz-Sandoval, S. Ganguli, A. K. Roy, D. J. Smith, R. Vajtai, B. G. Sumpter, V. Meunier, H. Terrones, M. Terrones and P. M. Ajayan, *Sci. Rep.*, 2012, **2**.
- 71 H. Wang, E. Wang, Z. Liu, D. Gao, R. Yuan, L. Sun and Y. Zhu, *Journal of Materials Chemistry A*, 2015, **3**, 266-273.
- 72 B. Ge, Z. Zhang, X. Zhu, X. Men and X. Zhou, *Colloids and Surfaces A: Physicochemical and Engineering Aspects*, 2014, **457**, 397-401.
- 73 C.-F. Wang and S.-J. Lin, *ACS Applied Materials & Interfaces*, 2013, **5**, 8861-8864.
- 74 K. C. Kemp, H. Seema, M. Saleh, N. H. Le, K. Mahesh, V. Chandra and K. S. Kim, *Nanoscale*, 2013, **5**, 3149-3171.
- 75 H.-P. Cong, J.-F. Chen and S.-H. Yu, *Chemical Society Reviews*, 2014, **43**, 7295-7325.
- 76 Z. Chen, L. Dong, D. Yang and H. Lu, *Advanced Materials*, 2013, **25**, 5352-5359.
- 77 M. Fang, Z. Tang, H. Lu and S. Nutt, *Journal of Materials Chemistry*, 2012, **22**, 109-114.
- 78 L.-W. Tsai and N.-H. Tai, *ACS Applied Materials & Interfaces*, 2014, **6**, 10489-10496.
- 79 Y. Chen, Y. Li, M. Yip and N. Tai, *Composites Science and Technology*, 2013, **80**, 80-86.
- 80 A. Chakrabarti, J. Lu, J. C. Skrabutenas, T. Xu, Z. Xiao, J. A. Maguire and N. S. Hosmane, *Journal of Materials Chemistry*, 2011, **21**, 9491-9493.
- 81 D. V. Kosynkin, A. L. Higginbotham, A. Sinitskii, J. R. Lomeda, A. Dimiev, B. K. Price and J. M. Tour, *Nature*, 2009, **458**, 872-876.
- 82 H. Bi, X. Xie, K. Yin, Y. Zhou, S. Wan, L. He, F. Xu, F. Banhart, L. Sun and R. S. Ruoff, *Advanced Functional Materials*, 2012, **22**, 4421-4425.
- 83 M. Iqbal and A. Abdala, *Environ Sci Pollut Res*, 2013, **20**, 3271-3279.
- 84 J. Wang, Z. Shi, J. Fan, Y. Ge, J. Yin and G. Hu, *Journal of Materials Chemistry*, 2012, **22**, 22459-22466.
- 85 R. Li, C. Chen, J. Li, L. Xu, G. Xiao and D. Yan, *Journal of Materials Chemistry A*, 2014, **2**, 3057-3064.
- 86 D.-a. Zha, S. Mei, Z. Wang, H. Li, Z. Shi and Z. Jin, *Carbon*, 2011, **49**, 5166-5172.
- 87 H. Li, L. Liu and F. Yang, *Journal of Materials Chemistry A*, 2013, **1**, 3446-3453.
- 88 X. Song, L. Lin, M. Rong, Y. Wang, Z. Xie and X. Chen, *Carbon*, 2014, **80**, 174-182.
- 89 T. Wu, M. Chen, L. Zhang, X. Xu, Y. Liu, J. Yan, W. Wang and J. Gao, *Journal of Materials Chemistry A*, 2013, **1**, 7612-7621.
- 90 G. Wei, Y.-E. Miao, C. Zhang, Z. Yang, Z. Liu, W. W. Tjiu and T. Liu, *ACS Applied Materials & Interfaces*, 2013, **5**, 7584-7591.
- 91 H.-P. Cong, X.-C. Ren, P. Wang and S.-H. Yu, *ACS Nano*, 2012, **6**, 2693-2703.
- 92 J. Li, J. Li, H. Meng, S. Xie, B. Zhang, L. Li, H. Ma, J. Zhang and M. Yu, *Journal of Materials Chemistry A*, 2014, **2**, 2934-2941.
- 93 Y. Zhao, C. Hu, Y. Hu, H. Cheng, G. Shi and L. Qu, *Angewandte Chemie International Edition*, 2012, **51**, 11371-11375.
- 94 Y. He, Y. Liu, T. Wu, J. Ma, X. Wang, Q. Gong, W. Kong, F. Xing, Y. Liu and J. Gao, *Journal of Hazardous Materials*, 2013, **260**, 796-805.
- 95 Y. Liu, J. Zhou, E. Zhu, J. Tang, X. Liu and W. Tang, *Carbon*, 2015, **82**, 264-272.
- 96 Z. Niu, J. Chen, H. H. Hng, J. Ma and X. Chen, *Advanced Materials*, 2012, **24**, 4144-4150.
- 97 S. J. Yang, J. H. Kang, H. Jung, T. Kim and C. R. Park, *Journal of Materials Chemistry A*, 2013, **1**, 9427-9432.
- 98 D. D. Nguyen, N.-H. Tai, S.-B. Lee and W.-S. Kuo, *Energy & Environmental Science*, 2012, **5**, 7908-7912.
- 99 Y. Liu, J. Ma, T. Wu, X. Wang, G. Huang, Y. Liu, H. Qiu, Y. Li, W. Wang and J. Gao, *ACS Applied Materials & Interfaces*, 2013, **5**, 10018-10026.
- 100 H. Sun, Z. Zhu, W. Liang, B. Yang, X. Qin, X. Zhao, C. Pei, P. La and A. Li, *RSC Advances*, 2014, **4**, 30587-30591.
- 101 S. Ramasundaram, J. H. Jung, E. Chung, S. K. Maeng, S. H. Lee, K. G. Song and S. W. Hong, *Carbon*, 2014, **70**, 179-189.
- 102 H. Sun, A. Li, X. Qin, Z. Zhu, W. Liang, J. An, P. La and W. Deng, *ChemSusChem*, 2013, **6**, 2377-2381.
- 103 B. Li, X. Liu, X. Zhang, J. Zou, W. Chai and J. Xu, *Journal of Applied Polymer Science*, 2015, **132**, 41821.
- 104 B. Ge, Z. Zhang, X. Zhu, X. Men, X. Zhou and Q. Xue, *Composites Science and Technology*, 2014, **102**, 100-105.
- 105 C. Liu, J. Yang, Y. Tang, L. Yin, H. Tang and C. Li, *Colloids and Surfaces A: Physicochemical and Engineering Aspects*, 2015, **468**, 10-16.
- 106 H.-d. Liu, Z.-y. Liu, M.-b. Yang and Q. He, *Journal of Applied Polymer Science*, 2013, **130**, 3530-3536.
- 107 H. Bi, Z. Yin, X. Cao, X. Xie, C. Tan, X. Huang, B. Chen, F. Chen, Q. Yang, X. Bu, X. Lu, L. Sun and H. Zhang, *Advanced Materials*, 2013, **25**, 5916-5921.
- 108 B. Wang, R. Karthikeyan, X.-Y. Lu, J. Xuan and M. K. H. Leung, *Industrial & Engineering Chemistry Research*, 2013, **52**, 18251-18261.
- 109 Y.-Q. Li, Y. A. Samad, K. Polychronopoulou, S. M. Alhassan and K. Liao, *ACS Sustainable Chemistry & Engineering*, 2014, **2**, 1492-1497.
- 110 S. Huang and J. Shi, *Industrial & Engineering Chemistry Research*, 2014, **53**, 4888-4893.
- 111 H. Bi, X. Huang, X. Wu, X. Cao, C. Tan, Z. Yin, X. Lu, L. Sun and H. Zhang, *Small*, 2014, **10**, 3544-3550.
- 112 Z.-Y. Wu, C. Li, H.-W. Liang, J.-F. Chen and S.-H. Yu, *Angewandte Chemie International Edition*, 2013, **52**, 2925-2929.

- 113 Y. Men, M. Siebenburger, X. Qiu, M. Antonietti and J. Yuan, *Journal of Materials Chemistry A*, 2013, **1**, 11887-11893.
- 114 H. Wang, Y. Gong and Y. Wang, *RSC Advances*, 2014, **4**, 45753-45759.
- 115 Z.-Y. Wu, C. Li, H.-W. Liang, Y.-N. Zhang, X. Wang, J.-F. Chen and S.-H. Yu, *Sci. Rep.*, 2014, **4**.
- 116 Y. Yang, Z. Tong, T. Ngai and C. Wang, *ACS Applied Materials & Interfaces*, 2014, **6**, 6351-6360.
- 117 H. Hu, Z. Zhao, Y. Gogotsi and J. Qiu, *Environmental Science & Technology Letters*, 2014, **1**, 214-220.
- 118 X. Dong, J. Chen, Y. Ma, J. Wang, M. B. Chan-Park, X. Liu, L. Wang, W. Huang and P. Chen, *Chemical Communications*, 2012, **48**, 10660-10662.
- 119 S. Kabiri, D. N. H. Tran, T. Altalhi and D. Losic, *Carbon*, 2014, **80**, 523-533.
- 120 H. Sun, Z. Xu and C. Gao, *Advanced Materials*, 2013, **25**, 2554-2560.
- 121 M. Toyoda, K. Moriya, J.-i. Aizawa, H. Konno and M. Inagaki, *Desalination*, 2000, **128**, 205-211.
- 122 M. Inagaki, H. Konno, M. Toyoda, K. Moriya and T. Kihara, *Desalination*, 2000, **128**, 213-218.
- 123 M. Toyoda, J. Aizawa and M. Inagaki, *Desalination*, 1998, **115**, 199-201.
- 124 T. Wei, Z. Fan, G. Luo, C. Zheng and D. Xie, *Carbon*, 2009, **47**, 337-339.
- 125 A. Bayat, S. F. Aghamiri and A. Moheb, *Iranian Journal of Chemical Engineering*, 2008, **5**, 51-64.
- 126 G. Hristea and P. Budrugaec, *J Therm Anal Calorim*, 2008, **91**, 817-823.
- 127 M. Toyoda and M. Inagaki, *Carbon*, 2000, **38**, 199-210.
- 128 Y. Hu, X. Liu, J. Zou, T. Gu, W. Chai and H. Li, *ACS Applied Materials & Interfaces*, 2013, **5**, 7737-7742.
- 129 L. Wang, X. Fu, E. Chang, H. Wu, K. Zhang, X. Lei, R. Zhang, X. Qi and Y. Yang, *Journal of Chemistry*, 2014, **2014**, 5.
- 130 W. Dai, S. J. Kim, W.-K. Seong, S. H. Kim, K.-R. Lee, H.-Y. Kim and M.-W. Moon, *Sci. Rep.*, 2013, **3**.
- 131 Y. Gao, Y. S. Zhou, W. Xiong, M. Wang, L. Fan, H. Rabiee-Golgir, L. Jiang, W. Hou, X. Huang, L. Jiang, J.-F. Silvain and Y. F. Lu, *ACS Applied Materials & Interfaces*, 2014, **6**, 5924-5929.
- 132 N. Xiao, Y. Zhou, Z. Ling and J. Qiu, *Carbon*, 2013, **59**, 530-536.
- 133 B. Cortese, D. Caschera, F. Federici, G. M. Ingo and G. Gigli, *Journal of Materials Chemistry A*, 2014, **2**, 6781-6789.
- 134 H. Shi, D. Shi, L. Yin, Z. Yang, S. Luan, J. Gao, J. Zha, J. Yin and R. K. Y. Li, *Nanoscale*, 2014, **6**, 13748-13753.
- 135 Y. Zeng, K. Wang, J. Yao and H. Wang, *Carbon*, 2014, **69**, 25-31.

Journal of Materials Chemistry A

ARTICLE



Fig. 1 Spilled oil pollute on the beach of Kinmen county, Fujian province. Adopted with permission from Apple Daily²

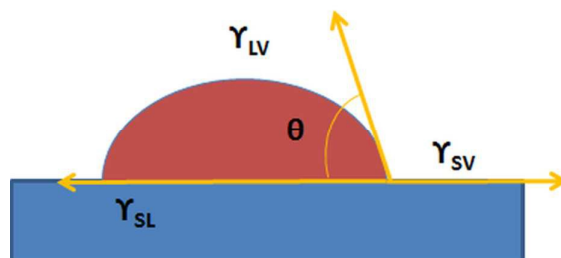


Fig. 2 A liquid drop on the flat surface.

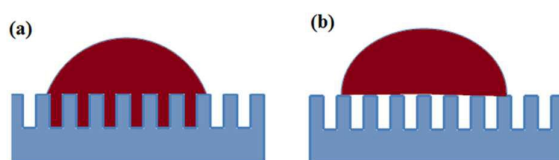


Fig. 3 (a) Wenzel state or homogeneous wetting on a hydrophobic, rough surface, (b) Cassie-Baxter state or heterogeneous wetting on a hydrophobic, rough surface.

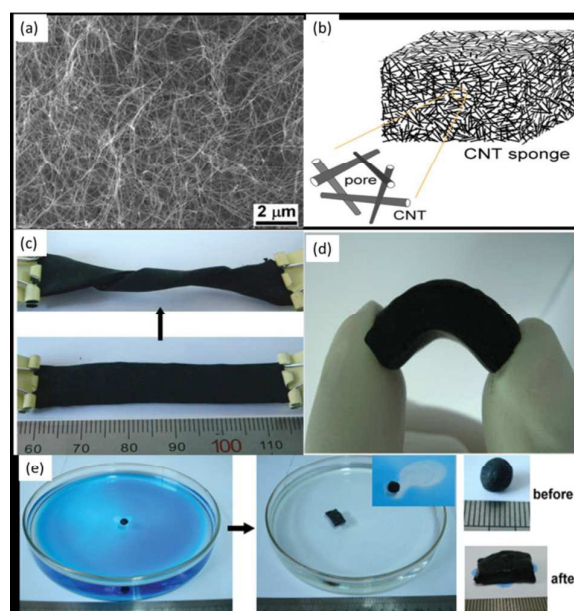


Fig. 4 (a) Cross-sectional SEM image of the CNTs sponge, (b) Depiction of sponge consisting CNT piles (black lines) as the skeleton and open pores (void space), (c) Twisting of sponge by three round turns at the ends without breaking, (d) Bending of CNT sponge at a large-angle, (e) Absorption of diesel oil film by CNT sponge. Inset shows that the size increased and shape becomes rectangular. Reprinted with permission from ref. 66. Copyright 2010 WILEY-VCH Verlag GmbH & Co. KGaA, Weinheim.

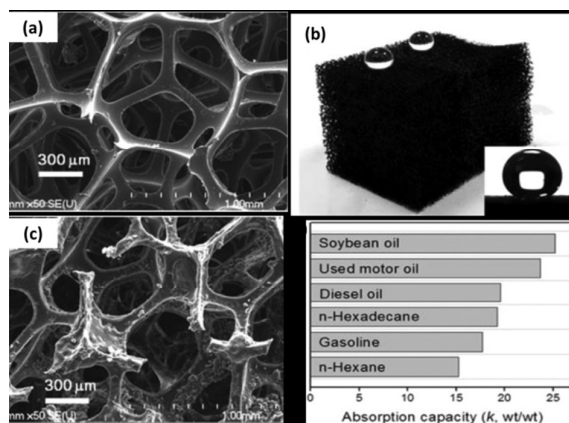


Fig. 5 (a) SEM image of PU sponge, (b) an optical image of the CNT/PDMS-coated PU sponge. Inset showing the superhydrophobic nature of the as-prepared sponge, (c) SEM images of PU sponge after CNT/ PDMS-coating and (d) Absorption capacities of the CNT/PDMS-coated PU sponge for different oil and organic solvents. Reprinted with permission from ref. 73. Copyright 2013 American Chemical Society

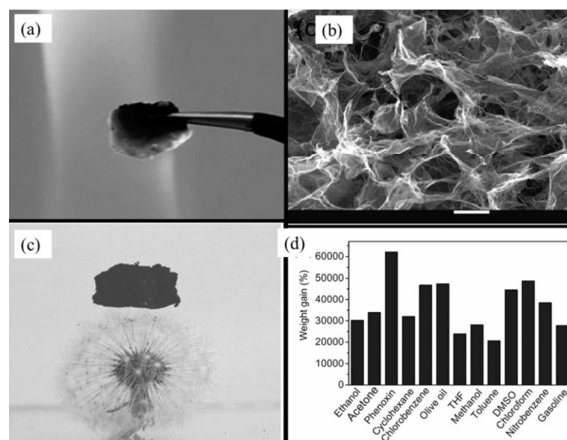


Fig. 6 (a) Fire-resistance property of GF, (b) SEM micrograph of a graphene framework, (c) Ultra-light GF of size 1.8 cm \times 1.1 cm \times 1.2 cm standing on a dandelion and (d) Absorption capacities of GF for different oil and organic solvents. Reprinted with permission from ref. 93. Copyright 2012 Wiley-VCH Verlag GmbH & Co. KGaA, Weinheim.

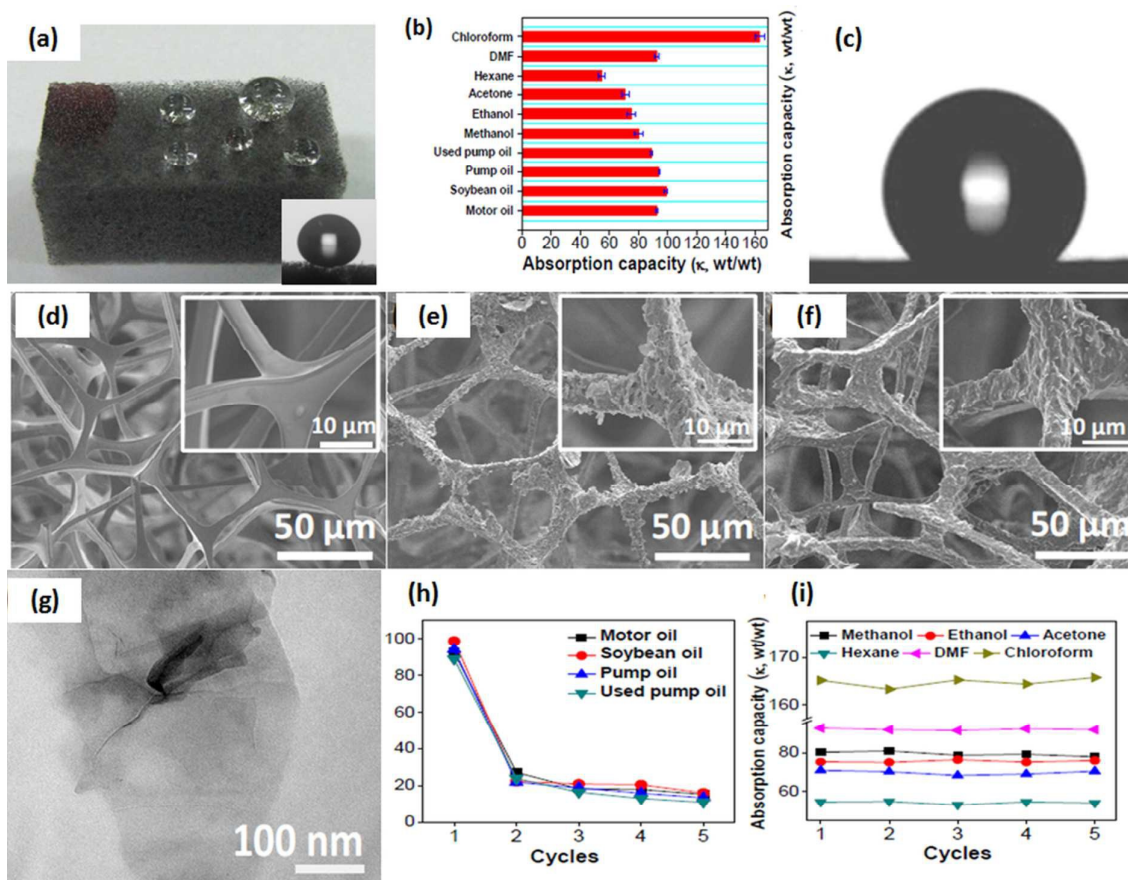


Fig. 7 (a) Graphene-PDMS coated sponge showing superhydrophobic and superoleophilic properties, (b) absorption capacity of the graphene-PDMS coated sponge for different oils, (c) graphene film showing water contact angle of 132° . FESEM images of (d) pure sponge (e) graphene loading of 7.3% on sponge, (f) sponge after graphene and PDMS coating. Insets: higher magnification FESEM images, (g) TEM image of graphene nanosheets. Recyclability of graphene-PDMS coated sponge for different (h) oils and (i) organic solvents. Reprinted with permission from ref. 98. Copyright 2012 The Royal Society of Chemistry.

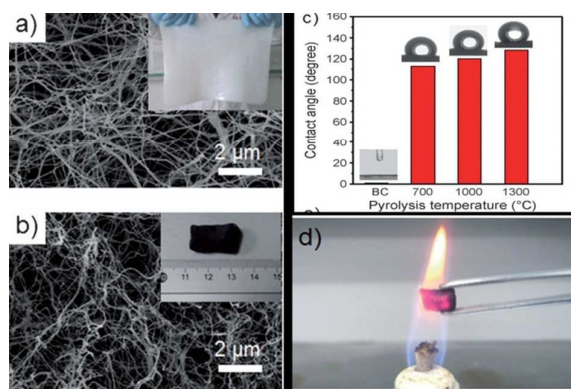


Fig. 8 SEM images of (a) the BC aerogel and (b) the CNF aerogel treated at 1300 °C. Insets: (a) and (b) show the photographs of the BC pellicle and the CNF aerogel prepared by pyrolysis at 1300 °C, (c) Effect of pyrolysis temperature on water contact angle and (d) Photograph of CNF aerogel in a hot flame of an alcohol burner. Reprinted with permission from ref. 112. Copyright 2013 Wiley-VCH Verlag GmbH & Co. KGaA, Weinheim.

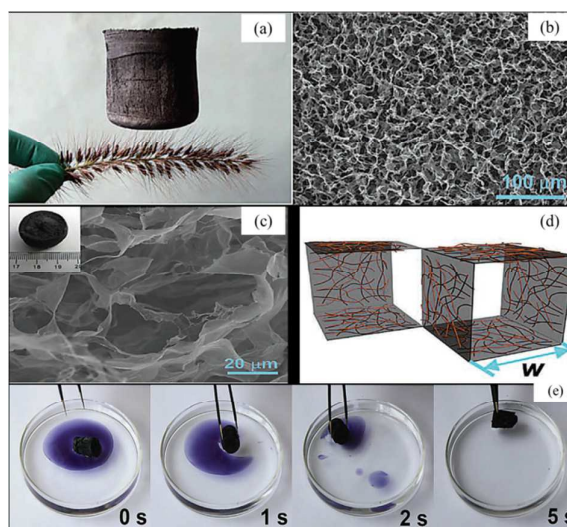


Fig. 9 (a) A 100 cm³ UFA cylinder standing on a flower like dog's tail, (b) an interconnected, porous three-dimensional (3D) framework of randomly oriented, crinkly sheets with continuous macropores ranged from hundreds of nanometers to tens of micrometers, (c) SEM image and photograph (inset in (c)) of the lightest neat graphene aerogel ($\rho = 0.16 \text{ mg cm}^{-3}$), (d) schematic illustration of idealized building cells of our UFA made by synergistic assembly of graphene and CNTs and (e) fast absorption process of toluene (stained with Sudan Black B) on water by the UFA within 5 s. Reprinted with permission from ref. 120. Copyright 2013 WILEY-VCH Verlag GmbH & Co. KGaA, Weinheim.

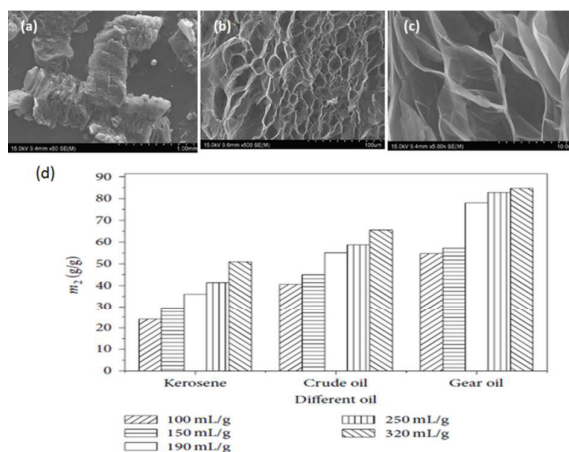


Fig. 10 SEM images of (a) worm-like MEG, (b) surface morphology of MEG, (c) the pore walls and (d) absorption capacity of MEG for different industrial oils with volume expansion. Reprinted with permission from ref. 129. Copyright 2014 LiqinWang et al.

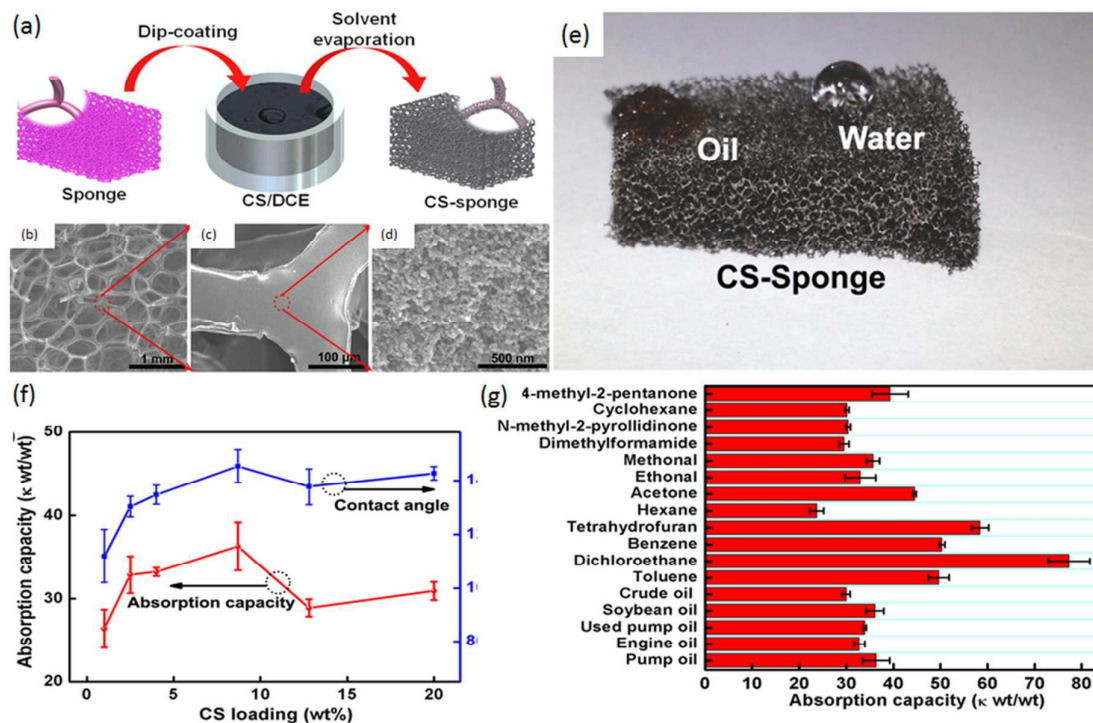


Fig. 11 (a) Schematic showing the dip coating process of CS on sponge. SEM images of (b) sponge before coating and (c, d) sponge after uniform coating of CS, (e) CS-sponge showing superoleophilic and superhydrophobic properties with water contact angle of 144°, (f) effect of CS loading on water contact angle and absorption capacity of pump oil and (g) absorption capacity of CS-sponge for different oil and organic solvent. Reprinted with permission from ref. 131. Copyright 2014 American Chemical Society.

Table 1 Brief description of the best performances of different carbon-based absorbents

Sorbent	Materials	Method	Density (mg/cm ³)	Water contact angle	Absorption capacity	Method of extraction	Ref.
Carbon nanotubes	1,2-dichlorobenzene, ferrocene powder	CVD	5–10	156	80-180	mechanical	66
CNTs coated sponges	PU sponge, Tris-HCl, CNTs, ODA, Anhydrous ethanol	self-polymerization	-	158	22-35	mechanical	71
Graphene	Graphene oxide, pyrrole	Hydrothermal followed by freezing drying and annealing	2.1 ± 0.3	-	200–600	-	93
Graphene coated sponges	melamine sponge, PDMS, graphene	dip coating	11.3	162	54 - 165	Mechanical squeezing	98
Carbon aerogel	Bacterial cellulose pellicles	freeze-drying followed by pyrolysis	4–6	128.64	106-312	distillation, direct combustion	112
Graphene-CNTs aerogel	GGO, CNTs	freeze-drying followed by chemical reduction	0.16-22.4	132.9	215-913	mechanical or heating	120
Graphite	natural graphite, H ₂ SO ₄ , HNO ₃ , KMnO ₄ or FeCl ₃	thermal expansion of H ₂ SO ₄ -graphite intercalation compound	3.9-25.7	-	2.4–9.7 L/100 g absorbent	-	126
Carbon Soot Sponge	ethylene, oxygen and melamine sponges	combustion flame method followed by dip-coating	-	144	25–80	heating	131
Carbon nanofibers/carbon foam composite	CLR, THF, polyurethane (PU) foam slabs	template synthesis of carbon foam and CCVD treatment	-	140	15-28	-	132
Carbonaceous nanoparticles modified polyurethane foam	Carbonaceous nanoparticles, PU foam	Ultrasonication	-	127.6	50-121	-	134
Hollow carbon beads	Polysulfone, N-methyl-2-pyrrolidone, tetraethyl orthosilicate, cetyltrimethylammoniumbromide, sodium hydroxide	simple phase inversion method and subsequent carbonisation	200	148	50–55% of their own volume	heat treatment	135